Dual inhibition of airway inflammation and fibrosis by common β cytokine receptor blockade

Hao Wang, PhD,[a]* Kwok Ho Yip, PhD,[b]* Simon P. Keam, PhD,[c] Ross Vlahos, PhD,[a] Kristy Nichol, PhD,[d,e] Peter Wark, MD, PhD,[d,e] John Toubia, PhD,[b] Anita C. Kral, BSc,[b] Gökhan Cildir, PhD,[b] Harshita Pant, BMBS, PhD,[b,f] Timothy R. Hercus, PhD,[b] Nick Wilson, PhD,[c] Catherine Owczarek, PhD,[c] Angel F. Lopez, MBBS, PhD,[b,f] Steven Bozinovski, PhD,[a]‡ and Damon J. Tumes, PhD[b]‡ *Bundoora, Adelaide, Parkville, and Newcastle, Australia*

Background: Patients with severe asthma can present with eosinophilic type 2 (T2), neutrophilic, or mixed inflammation that drives airway remodeling and exacerbations and represents a major treatment challenge. The common β (βc) receptor signals for 3 cytokines, GM-CSF, IL-5, and IL-3, which collectively mediate T2 and neutrophilic inflammation.
Objective: To determine the pathogenesis of βc receptor–mediated inflammation and remodeling in severe asthma and to investigate βc antagonism as a therapeutic strategy for mixed granulocytic airway disease.
Methods: βc gene expression was analyzed in bronchial biopsy specimens from patients with mild-to-moderate and severe asthma. House dust mite extract and *Aspergillus fumigatus* extract (ASP) models were used to establish asthma-like pathology and airway remodeling in human βc transgenic mice. Lung tissue gene expression was analyzed by RNA sequencing. The mAb CSL311 targeting the shared cytokine binding site of βc was used to block βc signaling.
Results: βc gene expression was increased in patients with severe asthma. CSL311 potently reduced lung neutrophils, eosinophils, and interstitial macrophages and improved airway pathology and lung function in the acute steroid-resistant house dust mite extract model. Chronic intranasal ASP exposure induced airway inflammation and fibrosis and impaired lung function that was inhibited by CSL311. CSL311 normalized the ASP-induced fibrosis-associated extracellular matrix gene expression network and strongly reduced signatures of cellular inflammation in the lung.
Conclusions: βc cytokines drive steroid-resistant mixed myeloid cell airway inflammation and fibrosis. The anti-βc antibody CSL311 effectively inhibits mixed T2/neutrophilic inflammation and severe asthma-like pathology and reverses fibrosis gene signatures induced by exposure to commonly encountered environmental allergens. (J Allergy Clin Immunol 2023;■■■:■■■-■■■.)

Key words: *Asthma, common β cytokine, CSL311, antibody, biologic, trabikibart, fibrosis, collagen, remodeling, airway, inflammation, hyperactivity, eosinophils, neutrophils, macrophages, IL-3, IL-5, GM-CSF*

Asthma is a chronic inflammatory disease of the lung characterized by reversible airway obstruction and remodeling of the conducting airways. While inhaled corticosteroids are highly effective in treating most patients with asthma, some patients experience severe disease because current treatments fail to manage their symptoms. Currently, limited treatment options are available for severe asthma, which primarily target specific mediators in the eosinophilic/T2 inflammation pathway.[1] Severe asthma can also result in a major shift in immunopathology, with up to 50% of patients with severe asthma presenting with neutrophil-dominant or mixed granulocytic inflammation rather than eosinophilic/T2 inflammation.[2,3] Therapeutics that block neutrophils (anti-IL-17 biologics and CXCR2 antagonists) have not translated into clinical benefit,[4,5] and no treatments directly target both neutrophils and eosinophils simultaneously. Further, in patients with severe T2-high asthma, treatment may be confounded by phenotype overlap (eg, high IgE and blood eosinophilia) and cytokine redundancy (eg, GM-CSF and IL-5), and optimal treatment outcomes may not be achieved with therapies that target a single molecule.[6] Hence, multitarget approaches may be necessary to treat complex diseases associated with excessive activation of multiple myeloid cell populations.

The common β (βc) cytokine family consists of 3 cytokines, GM-CSF, IL-3, and IL-5, which bind a heterodimeric receptor comprising a ligand-specific α chain and a dimer of βc that is shared by all 3 receptors.[7] The GM-CSF receptor α chain is ubiquitously expressed in macrophages, monocytes, eosinophils, and neutrophils and is important for their

From [a]the School of Health and Biomedical Sciences, RMIT University, Bundoora; [b]the Centre for Cancer Biology, SA Pathology and the University of South Australia, Adelaide; [c]Research and Development, CSL Limited, Bio21 Molecular Science and Biotechnology Institute, Parkville; [d]the Immune Health Research Program, Hunter Medical Research Institute and University of Newcastle, Newcastle; [e]the Department of Respiratory and Sleep Medicine, John Hunter Hospital, Newcastle; and [f]Faculty of Medicine, University of Adelaide, Adelaide.
*These authors contributed equally to this work as co-first authors.
‡These authors contributed equally to this work as co-senior authors.
Received for publication March 25, 2023; revised September 11, 2023; accepted for publication October 12, 2023.

Corresponding authors: Damon J. Tumes, PhD, Centre for Cancer Biology, SA Pathology and the University of South Australia, PO Box 2471, Adelaide, SA 5001, Australia. E-mail: damon.tumes@unisa.edu.au. Or: Steven Bozinovski, PhD, School of Health and Biomedical Sciences, RMIT University, PO Box 71, Bundoora, VIC 3083, Australia. E-mail: steven.bozinovski@rmit.edu.au.
0091-6749

https://doi.org/10.1016/j.jaci.2023.10.021

Abbreviations used
ACQ: Asthma Control Questionnaire
AHR: Airway hyperresponsiveness
ASP: *Aspergillus fumigatus* extract
BAL: Bronchoalveolar lavage
BALF: Bronchoalveolar lavage fluid
βc: Common β
dsDNA: Double-stranded DNA
ECM: Extracellular matrix
GINA: Global Initiative for Asthma
GSEA: Gene set enrichment analysis
hβc: Human common β
hβcTg: Human βc transgenic
HDM: House dust mite extract
MT: Masson trichrome
NET: Neutrophil extracellular trap

functional development. IL-3 receptor α subunit is expressed by mast cells, dendritic cells, endothelial cells, and basophils, while IL-5 receptor α subunit is expressed mainly by basophils and eosinophils.[8,9] CSL311 is a fully human mAb that competitively binds to the common cytokine binding site of human common β (hβc), the major signaling subunit of the GM-CSF, IL-5, and IL-3 receptors.[10] The action of CSL311 has been characterized in our previous work,[10-13] but its ability to inhibit severe and steroid-resistant asthma and associated lung fibrosis is yet to be studied.

In this study, we analyzed expression of βc (*CSF2RB*) in bronchial biopsy specimens of patients with asthma stratified based on disease severity. Furthermore, we used a novel transgenic mouse model engineered to express the hβc receptor instead of mouse βc receptors, referred to herein as human βc transgenic (hβcTg) mice[12] to block hβc signaling in acute steroid-resistant and chronic asthma models featuring mixed-granulocytic airway inflammation, airway fibrosis, and airway hyperresponsiveness (AHR). Blocking hβc signaling markedly reduced immunopathology, AHR, and fibrotic lung remodeling in preclinical models and asthma that displayed mixed granulocytic inflammation.

METHODS

Asthma cohort analysis

Gene expression of *CSF2RB* and procollagen *COL1A1* was measured in bronchial biopsy specimens from a cohort of patients with asthma (n = 26; 12 with mild-to-moderate asthma and 14 with severe asthma) classified by Global Initiative for Asthma (GINA) definitions.[14] Patient characteristics are presented in Table I.

Animals

All animal experiments undertaken received RMIT University ethics approval and University of South Australia ethics approval in accordance with the guidelines of Animal Research: Reporting of *In Vivo* Experiments and National Health and Medical Research Council of Australia. Transgenic mice devoid of murine βc/βIL-3 receptors and expressing the hβc receptor (hβcTg mice) were used in this study, which respond to mouse GM-CSF and IL-5, but not IL-3, as previously described.[12]

TABLE I. Patient characteristics

Characteristic	Mild-to-moderate asthma (n = 12)	Severe asthma (n = 14)
Neutrophilic asthma, n (%)	5 (42)	7 (50)
Eosinophilic asthma, n (%)	2 (17)	6 (43)
Paucigranulocytic asthma, n (%)	5 (42)	1 (7)
Age, y, median (IQR)	57 (48-76)	63 (38-78)
Sex, male/female, n	6/6	5/9
Atopy, n (%)	6 (50)	8 (57)
FEV_1 % predicted, median (IQR)	79.5 (69.0-104.0)	75.5 (58.0-108.0)
ACQ score, median (IQR)	1.2 (0-2.2)	2.3 (1.2-3.5)
Positive bacterial culture, n (%)	4 (33.3)	10 (71.4)
BAL % neutrophils, median (range)	52.8 (1.5-94.0)	65.3 (17.5-96.0)
BAL % eosinophils, median (range)	1.4 (0.3-28.3)	1.9 (0.5-47.3)

IQR, Interquartile range.

Mouse airway inflammation and fibrosis models

To model steroid-refractory severe asthma, 8- to 12-week-old female hβcTg mice were sensitized with subcutaneous injection of 100 μg of house dust mite extract (HDM) (*Dermatophagoides pteronyssinus*; Stallergenes Greer, Lenoir, NC) in CFA (Sigma-Aldrich, St Louis, Mo). Mice were further challenged 8 days later with intranasal administration of 25 μg of HDM for 4 consecutive days. A human mAb against βc (CSL311; CSL Ltd, Melbourne, Victoria, Australia) or matching isotype control (BM4 clone; CSL Ltd) (50 mg/kg) was therapeutically administered intravenously via the tail vein on day 8 and day 10 before the HDM challenge. Mice were analyzed 24 hours after the last HDM challenge. For the chronic *Aspergillus fumigatus* extract (ASP) exposure model, mice were treated with 50 μg of ASP (item XPM3D3A25, lot 365084; Stallergenes Greer) once a week for 4 weeks followed by 20 μg of ASP twice a week for 4 weeks as described previously.[15] Isotype and CSL311 groups received intravenous injection of antibody (50 mg/kg) for the final 4 weeks. Mice were analyzed 48 hours after the last ASP challenge.

Data analysis

All data were analyzed using GraphPad Prism 9 (GraphPad Software, Boston, Mass). Animal data are presented as the mean ± SEM. Where detailed and appropriate, unpaired Student *t* test, one-way analysis of variance with Sidak or Bonferroni post hoc test, or Pearson correlation was performed. Nonparametric data from the clinical samples is reported as median (interquartile range) and was analyzed by Mann-Whitney test or Spearman correlation. $P < .05$ is considered to be statistically significant. Gene set enrichment analysis (GSEA) analysis (GSEA v4.3.2; https://www.gsea-msigdb.org/gsea/index.jsp) was performed using GSEA and default parameters in a ranked list analysis. Raw analysis data and output were visualized using RStudio (Posit Software, Boston, Mass) with ggplot2 v3.3.6 (https://cran.r-project.org/web/packages/ggplot2/index.html).

See additional methods in this article's Methods section in the Online Repository at www.jacionline.org.

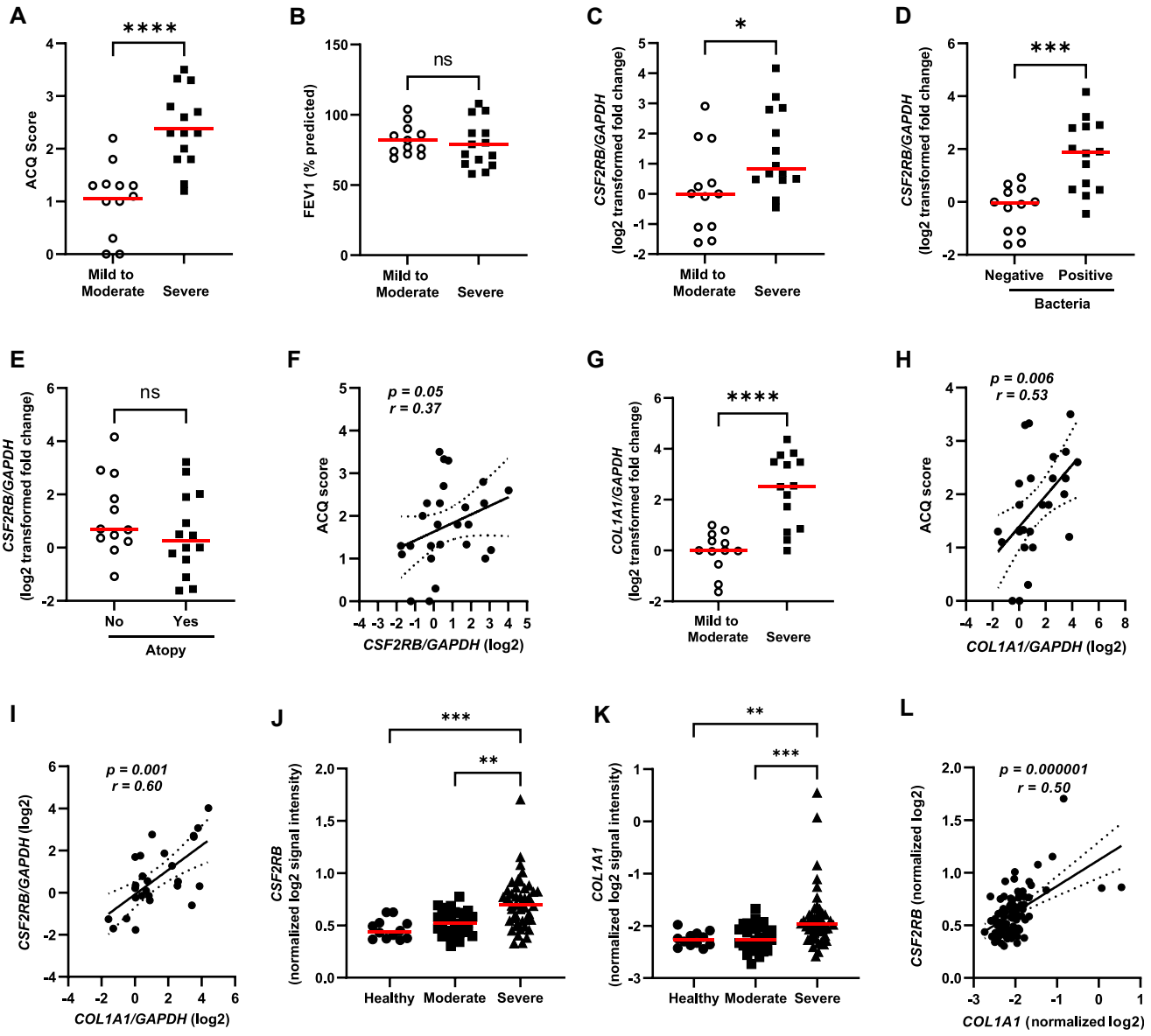

FIG 1. Expression of *CSF2RB* and *COL1A1* is increased in the lungs of patients with severe asthma. **(A-C)** Bronchial biopsy specimens were collected from a cohort of asthma patients classified according to the GINA guidelines into mild-to-moderate and severe groups. Patient ACQ scores *(A)*, patient FEV_1 (% predicted) *(B)*, and *CSF2RB* mRNA expression *(C)* are shown. **(D-F)** *CSF2RB* mRNA expression in bronchial biopsy specimens was further analyzed in patients based on bacterial detection status *(D)* or atopy status *(E)* and correlation with ACQ score *(F)*. **(G-I)** *COL1A1* mRNA expression was measured in bronchial biopsy specimens and compared in mild-to-moderate and severe groups *(G)* and assessed for correlation with ACQ scores *(H)* and *CSF2RB* mRNA expression *(I)*. **(J-L)** *CSF2RB (J)* and *COL1A1 (K)* mRNA expression was also assessed in BAL cells of asthma patients (GSE74986) and subjected to correlation analysis *(L)*. Analysis includes nonparametric Mann-Whitney *U* test *(A-E* and *G)*, Kruskal-Wallis test *(J* and *K)*, and Spearman correlation *(D, F, G, I,* and *L)*. Data are expressed as individual data points with median. $*P < .05$, $**P < .01$, $***P < .001$, $****P < .0001$. *ns*, Not significant.

RESULTS

Gene expression of *CSF2RB* and *COL1A1* was increased in lungs of patients with severe asthma

Bronchial biopsy specimens collected from a cohort of patients with asthma as previously reported[14] were used to quantify the mRNA expression of the βc receptor gene *CSF2RB*. Asthma Control Questionnaire (ACQ) scores were confirmed to be significantly increased in patients with severe asthma, which is consistent with the GINA definition of asthma severity (Fig 1, *A*). In contrast, FEV_1 was not significantly altered in patients with severe asthma (Fig 1, *B*), which is also consistently reported. There was a 2-fold increase in *CSF2RB* expression in patients with severe asthma compared with patients with mild-to-moderate asthma ($P < .05$) (Fig 1, *C*). *CSF2RB* gene expression was also significantly higher in asthmatic patients with positive bacterial culture (3-fold, $P < .0001$) (Fig 1, *D*), but not in asthmatic

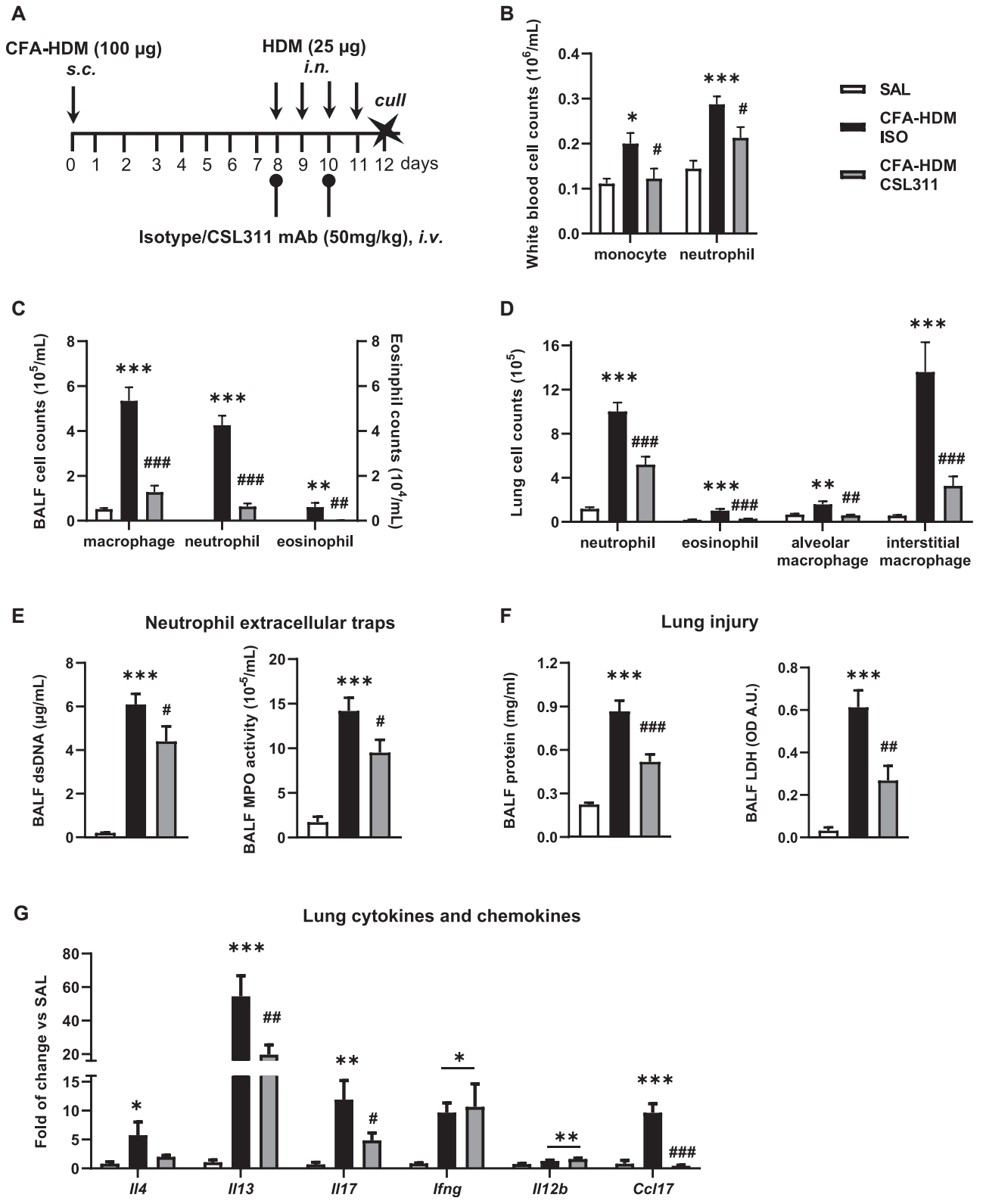

FIG 2. CFA-HDM-treated hβcTg mice demonstrate a mixed granulocytic lung inflammation, which was reduced by βc antagonism. **(A)** Schematic of CFA-HDM model and treatment regimen. **(B)** Blood monocytes and neutrophils were analyzed using CellDyn Emerald, and **(C)** BAL cell differentials were enumerated. **(D)** Lung neutrophils, eosinophils, alveolar macrophages, and interstitial macrophages were analyzed by flow cytometry. **(E)** Levels of dsDNA *(left panel)* and myeloperoxidase activity *(right panel)* in BALF were measured as NET markers. **(F)** Total protein *(left panel)* and lactate dehydrogenase *(right panel)* in BALF were measured as lung injury markers. **(G)** Frozen lungs were subjected to quantitative RT-PCR analysis

patients with atopy (Fig 1, *E*), and was positively associated with ACQ scores ($P = .05$) (Fig 1, *F*). Of interest, expression of procollagen gene *COL1A1* was increased in patients with severe asthma by 6-fold compared with patients with mild-to-moderate disease ($P < .0001$) (Fig 1, *G*), and this expression was positively correlated with both worse asthma symptoms (high ACQ score) and high *CSF2RB* expression (both $P < .01$) (Fig 1, *H* and *I*). Furthermore, in bronchoalveolar lavage (BAL) cells (data from GSE74986), *CSF2RB* and *COL1A1* transcripts were also found to be elevated in patients with severe asthma relative to both patients with moderate asthma and healthy control subjects (Fig 1, *J* and *K*), and a positive correlation was detected between *CSF2RB* and *COL1A1* expression (Fig 1, *L*).

Blockade of hβc by CSL311 reduced lung inflammation in a mouse model of severe asthma

To investigate the role of βc signaling in airway inflammation and pathology in vivo, we first evaluated the role of βc signaling in an established preclinical model of severe asthma[16] using hβcTg mice and therapeutically administering the CSL311 antibody to block hβc signaling during the HDM challenge phase (Fig 2, *A*). In mice treated with HDM and isotype control antibody, a systemic inflammatory response consisting of increased blood monocytes and neutrophils was detected (Fig 2, *B*) compared with saline-treated control mice. This response was accompanied by BAL inflammation dominated by infiltrating macrophages, neutrophils, and eosinophils (Fig 2, *C*). In lung tissue, leukocyte ($CD45^+$) infiltration was also observed with significant increases in neutrophils ($Ly6G^{high}CD11b^+$), eosinophils ($F4/80^+CD11c^{low}SiglecF^{high}$), alveolar macrophages ($F4/80^+CD11c^{high}SiglecF^{high}$), and monocyte-derived interstitial macrophages ($F4/80^+CD11c^+CD11b^+$) (Fig 2, *D*). Remarkably, CSL311 effectively prevented the expansion of blood monocytes and neutrophils (Fig 2, *B*) and significantly reduced BAL and lung infiltration of all types of leukocytes measured (Fig 2, *C* and *D*). In CFA-HDM isotype–treated mice, markers of neutrophil extracellular traps (NETs), double-stranded DNA (dsDNA) and myeloperoxidase, and markers of lung injury, bronchoalveolar lavage fluid (BALF) protein and lactate dehydrogenase, were detected, all of which were reduced by CSL311 (Fig 2, *E* and *F*). T_H2/T_H17 cytokines *Il4, Il13,* and *Il17* were induced by CFA-HDM and suppressed by CSL311, whereas T_H1 cytokines *Ifng* and *Il12b* induced by CFA-HDM were preserved in CSL311- treated mice (Fig 2, *G*). T-cell chemokine *Ccl17* induced by CFA-HDM was also suppressed by CSL311 (Fig 2, *G*).

Blockade of hβc by CSL311 reduced AHR and airway fibrosis in a mouse model of severe asthma

We further assessed the respiratory mechanics of the CFA-HDM-treated hβcTg mice. AHR was apparent after CFA-HDM treatment with increases in total respiratory system resistance after aerosol methacholine challenge (Fig 3, *A* and *B*), which were abolished by CSL311. At baseline, CFA-HDM treatment led to a downward shift in the pressure-volume curve (Fig 3, *C*) as well as reduction in quasi-static compliance (Fig 3, *D*) and an increase in respiratory system elastance (Fig 3, *E*), demonstrating a restrictive respiratory pattern that is suggestive of tissue stiffness and pulmonary fibrosis.[17,18] Consistently, CSL311 partially rescued this baseline lung function abnormality (Fig 3, *C-E*). Underlying these functional alternations, marked histopathology associated with peribronchiolar and alveolar inflammation was detected in CFA-HDM-treated mice (Fig 3, *F* and *H*). Masson trichrome (MT)–stained lung tissue sections also identified larger regions of intense collagen staining around their airways (Fig 3, *G* and *I*). A significant increase in the expression of type I collagen gene (*Col1a1*) (Fig 3, *J*) further supported the establishment of pulmonary fibrosis in CFA-HDM-treated mice. In line with the improvements in lung function, CSL311 significantly reduced alveolar and peribronchiolar inflammation and airway fibrosis (Fig 3, *G* and *I*). Lung expression of *Col1a1* was also reduced to control levels (Fig 3, *J*).

Airway remodeling is inhibited by CSL311 following chronic ASP challenge

To further investigate the role of βc signaling in asthma and fibrosis in response to chronic allergen exposure, we used an established chronic model of airway inflammation involving sensitization of mice by intranasal administration of 50 μg of ASP once a week for 4 weeks followed by intranasal administration of 20 μg of ASP twice a week for an additional 4 weeks.[15] Chronic ASP exposure induces airway remodeling and a mixed lymphocytic and granulocytic lung infiltrate consisting of both eosinophils and neutrophils.[15] To investigate the effect of blocking hβc, we administered CSL311 intravenously for the last 4 weeks of the model (Fig 4, *A*). Exposure to ASP induced fibrosis-associated changes in lung function including increased respiratory system elastance, static compliance, and associated pressure volume curves. CSL311 was again able to rescue ASP-associated lung function changes, returning their values to those similar to saline-treated animals (Fig 4, *B-D*). We next assessed visual changes to the airway using microscopy analysis of MT staining of lung sections. Tissue inflammation was induced by ASP and was significantly inhibited by CSL311 (Fig 4, *E* and *F*). ASP exposure also induced remodeling and increased collagen content around the conducting airways (Fig 4, *G*), which were strongly inhibited by CSL311 (Fig 4, *G* and *H*). We next compared the action of CSL311 with neutralizing antibodies against mouse IL-5 and mouse GM-CSF. ASP again induced peribronchial and alveolar cellular inflammation that was inhibited by CSL311, but not by anti-IL-5 or anti-GM-CSF alone (Fig E1, *A* and *B*, in the Online Repository at www.jacionline.org). Interestingly, CSL311 reduced both bronchiolar lavage eosinophils and neutrophils, whereas anti-IL-5 tended to reduce eosinophils ($P = .053$), but not neutrophils, and anti-GM-CSF reduced neutrophils ($P = .042$), but not eosinophils (Fig E1, *C*). ASP-

to measure mRNA expression of T_H2/T_H17 cytokines *Il4, Il13,* and *Il17*; T_H1 cytokines *Ifng* and *Il12b*; and T-cell chemokine *Ccl17*. n = 9 per group. Data are expressed as mean ± SEM. $*P < .05$, $**P < .01$, $***P < .001$ ISO vs SAL and $\#P < .05$, $\#\#P < .01$, $\#\#\#P < .001$ ISO vs CSL311 by one-way analysis of variance. *A.U.*, Arbitrary units; *i.n.*, intranasal; *ISO*, isotype; *i.v.*, intravenous; *LDH*, lactate dehydrogenase; *OD*, optical density; *SAL*, saline; *s.c.*, subcutaneous.

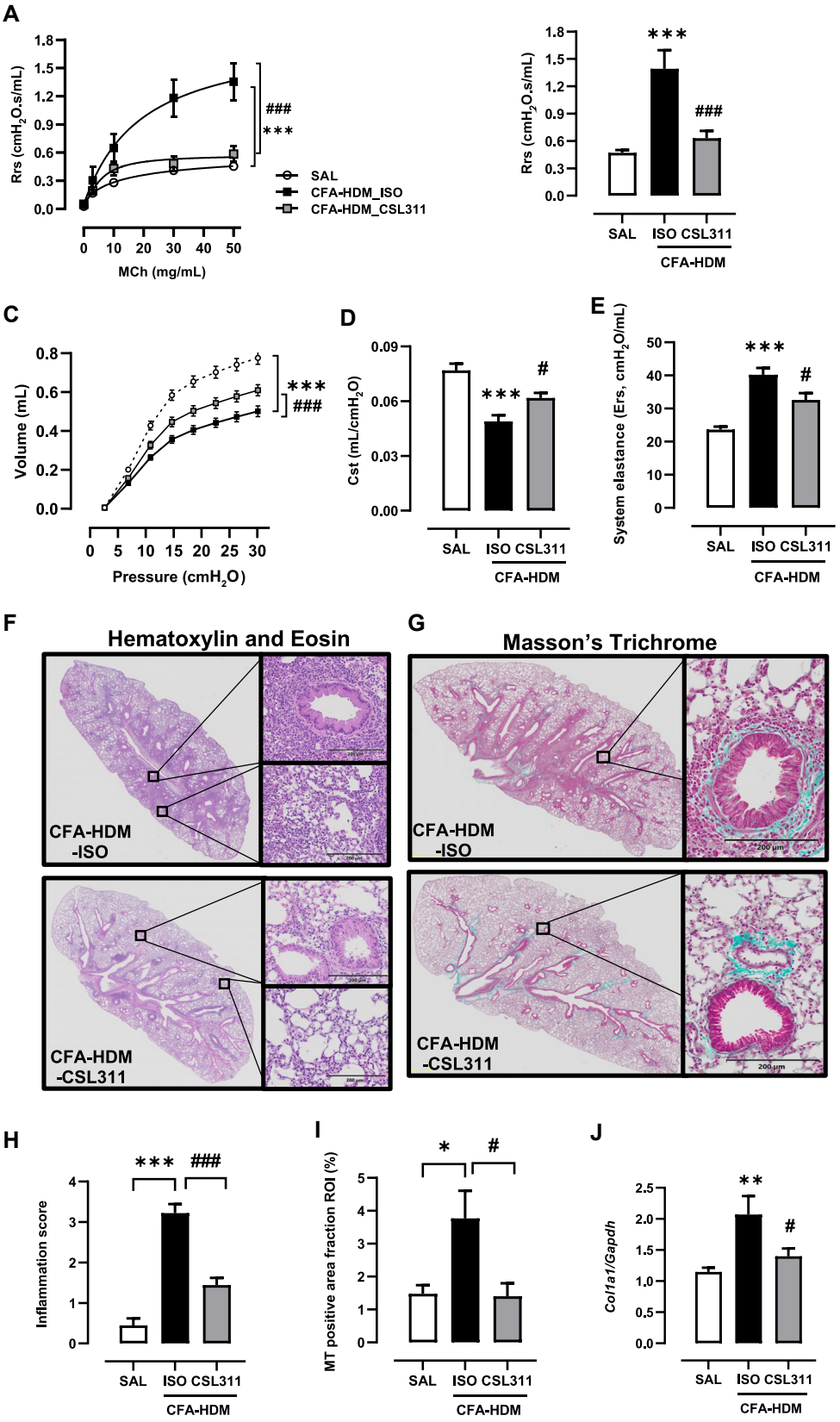

FIG 3. CFA-HDM-treated hβcTg mice develop AHR and airway fibrosis, which were reversed by βc antagonism. Respiratory mechanics were measured in anesthetized mice using flexiVent FX1, where baseline lung function parameters were first obtained, followed by additional measurements in response to increasing concentrations of nebulised methacholine. **(A** and **B)** Dose-response curves of respiratory system

induced collagen deposition was again reduced by CSL311, but not by either anti-IL-5 or anti-GM-CSF alone (Fig E1, *D* and *E*). Overall, these data indicate that CSL311 effectively blocks both airway inflammation and remodeling, which is more effective than blocking individual cytokines alone.

CSL311 results in global normalization of gene expression and extracellular matrisome signatures in ASP-challenged mice

To obtain further insight into the inflammatory pathways and structural changes in the lung that were inhibited by CSL311, we performed RNA sequencing on lung tissue from groups of saline-treated control hβcTg mice, ASP isotype–treated hβcTg mice, and ASP CSL311–treated hβcTg mice. ASP treatment resulted in upregulation of 728 genes and downregulation of 315 genes. Intravenous administration of CSL311 to ASP-treated mice resulted in 459 genes differentially regulated, with the majority (432 genes) downregulated (Fig 5, *A*). Of the 670 genes upregulated by ASP treatment, 268 were downregulated by CSL311, indicating that CSL311 broadly inhibits ASP-associated changes in gene expression (Fig 5, *B*). The effect of CSL311 on gene expression is depicted as a volcano plot with downregulated genes in blue and upregulated genes in orange (Fig 5, *C*). Of the ASP upregulated genes that were downregulated by CSL311, the most enriched Kyoto Encyclopedia of Genes and Genomes pathway[19] was cytokine-cytokine receptor interaction (31 genes, $P = 1.3 \times 10^{-14}$). The top gene ontology biological process was the immune system process (50 genes, $P = 4.2 \times 10^{-27}$) followed by adaptive immune response (35 genes, $P = 2.9 \times 10^{-23}$) and positive regulation of T-cell activation (13 genes, $P = 3.4 \times 10^{-14}$). The genes enriched in these biological processes consisted primarily of genes encoding surface receptors including *Cd3d, Cd4,* and *Cd8a* that are expressed on T cells and the accessory molecule *Cd79a* that is expressed on B cells; several MCH class II genes; and the antigen-presenting cell–expressed costimulatory molecule *CD86*. Of note, *Arg1* and *Chil3,* markers of M2 macrophages, and *Ear2* and *Prg2,* which are highly expressed by eosinophils, were also decreased by CSL311 treatment. Notably, *Ccr4* that is highly expressed by T_H2 and T_H17 cells was also increased by ASP and reduced by CSL311, accompanied by the same pattern of expression for the CCR4 ligand gene *Ccl17*. Prediction of cell types from the gene signatures using xCell[20] analysis also indicated that T_H2 cells and dendritic cell signatures were decreased following CSL311 treatment (Fig E2 in the Online Repository at www.jacionline.org). GSEA further demonstrated the marked dependency of βc signaling for inflammation following ASP exposure with strong enrichment of the hallmark inflammatory response gene set among the genes downregulated by CSL311 (Fig 5, *D*). Identification of differentially regulated gene modules using IPA (Qiagen, Hilden, Germany) showed that T_H1, T_H2, and IL-17 signaling pathways were enriched in the ASP-challenged isotype–treated group compared with the saline-challenged control group. In contrast, when we compared the ASP-challenged CSL311–treated group with the saline-challenged control group, activation of these pathways was not observed (T_H2 and IL-17 signaling) or was lessened (T_H1). Comparison of the ASP-challenged isotype–treated group with the ASP-challenged CSL311–treated group confirmed that IL-17 signaling was significantly reduced by inhibition of βc signaling (Fig 5, *E*).

Abnormal extracellular matrix (ECM) deposition is one of the main pathological processes that results in tissue remodeling and fibrosis, and our analysis indicates that blocking βc strongly inhibits ASP-induced airway remodeling and changes in airflow indicative of loss of airway tissue compliance (Fig 4). To investigate how CSL311 protects against airway remodeling, we next identified which ECM components were altered by ASP exposure and CSL311 treatment using gene sets derived from the matrisome project database.[21,22] We found that CSL311 significantly reduced ASP-induced changes to the lung tissue ECM signature and that the effect was most evident for ECM regulators and matrisome-associated genes (Fig 6, *A*). Unsupervised hierarchical clustering of the matrisome genes shows that the ASP-induced ECM regulatory program is largely normalized toward that in saline-challenged animals following treatment with CSL311 (Fig 6, *B*) with both ASP-upregulated (green module) and ASP-downregulated (blue module) genes returned to levels more similar to saline-treated animals. GSEA analysis of these gene sets confirmed that both ECM regulators and matrisome-associated genes were strongly enriched in the CSL311-downregulated gene list (Fig 6, *C*) and included *Mmp12* and *Mmp13* and *Tgfb1* and *Thbs4* (Fig 6, *D*). Of the 744 known ECM components and ECM regulators in the matrisome database, approximately 8% were upregulated (59 genes) and approximately 8% were downregulated (64 genes), and in each case the majority of these were significantly rescued (toward levels detected in saline-challenged mice) by CSL311. Interestingly, there was a positive enrichment of genes in both core matrisome and collagen gene signatures in CSL311-treated animals, indicating that some ECM signatures were also increased by CSL311. Further interrogation of the collagen gene signature showed that a discrete set of collagen genes was expressed in the ASP isotype group compared with the ASP CSL311 group (Fig 6, *E*, and Fig E3 in the Online Repository at www.jacionline.org). Notably, ASP exposure was associated with expression of collagen genes that encoded exclusively fibril-forming collagen species (10/10 genes) (Fig E3). In contrast, treatment of ASP-exposed mice with CSL311 was associated with expression of collagen genes that encoded mostly non-fibril-forming collagen species (6/8

resistance *(A)* and maximum respiratory system resistance *(B)* were assessed after methacholine challenge. **(C-E)** Changes in baseline pressure-volume curve *(C)* with reduced static compliance *(D)* and increased respiratory system elastance *(E)* after CSL311 treatment were demonstrated. **(F** and **G)** Lung sections were stained with hematoxylin and eosin *(F)* or MT *(G)* and scanned with a VS-120 Olympus slide scanner and analyzed with cellSens Dimension software. **(H** and **I)** Inflammation score *(H)* and collagen-positive area *(I)* around the airways were quantified. **(J)** mRNA expression of *Col1a1* in mouse lung tissue was measured by quantitative RT-PCR. n = 9 per group. Data are expressed as mean ± SEM. *$P < .05$, **$P < .01$, ***$P < .001$ ISO vs SAL and #$P < .05$, ###$P < .001$ ISO vs CSL311 by one-way analysis of variance. *Cst*, Static compliance; *Ers*, respiratory system elastance; *ISO*, isotype; *Mch*, methacholine; *ROI*, region of interest; *Rrs*, respiratory system resistance; *SAL*, saline.

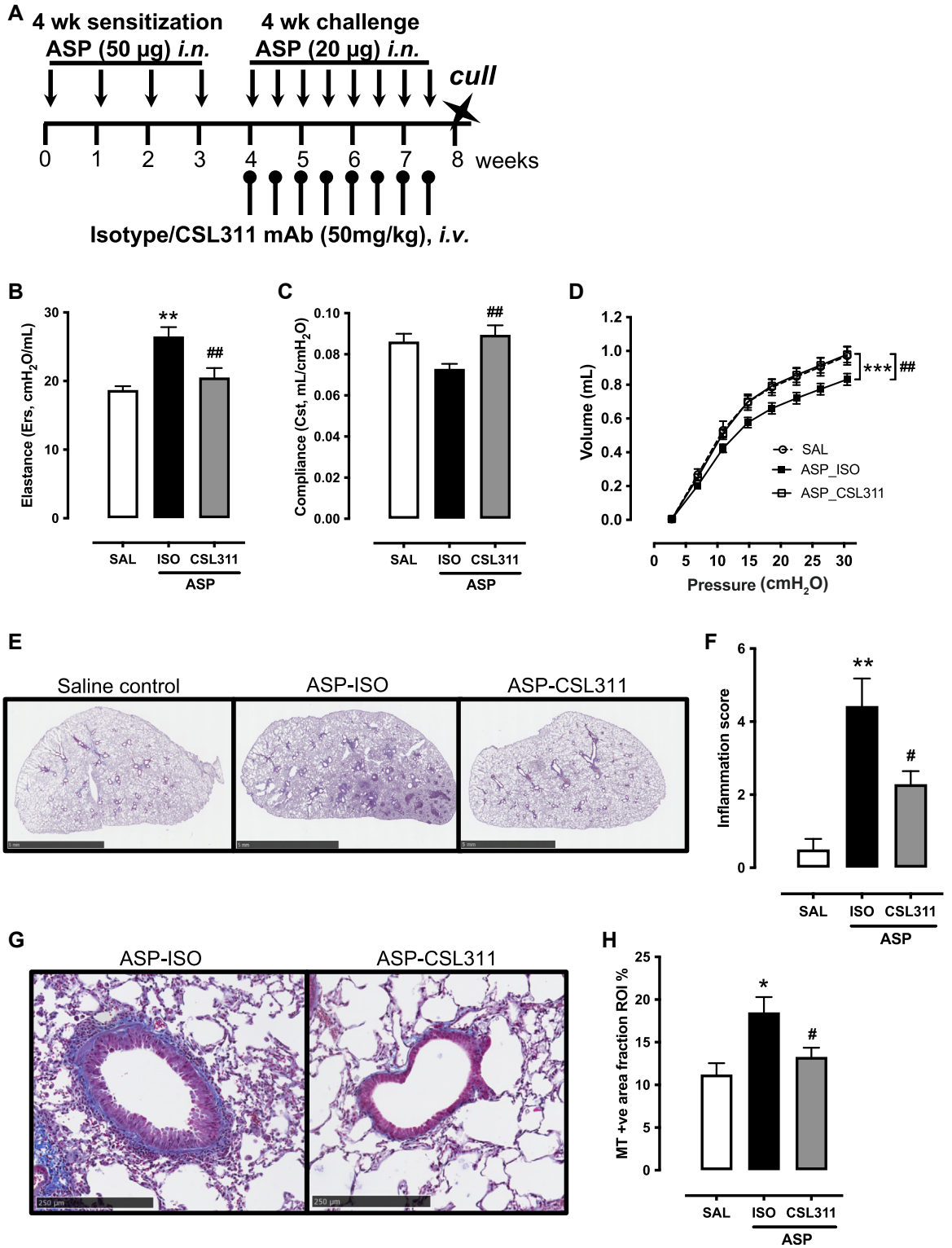

FIG 4. Chronic intranasal ASP challenge induces airway inflammation, impaired airway function, and remodeling that is reduced by βc antagonism. **(A)** Schematic of ASP model and treatment regimen. At 48 hours after the last ASP challenge, tracheotomy was done on the mice, and airway function assessed using mechanical ventilation with a flexiVent. **(B-D)** Measurement of respiratory system elastance *(B)*, static compliance *(C)*, and pressure-volume curves *(D)*. **(E)** Whole-lung lobe images of tissue sections stained with MT. **(F)** Inflammation score. **(G)** Airway tissue stained with MT in which collagen is stained blue. **(H)** Quantitation of collagen positive pixels. n = 3 SAL, n = 7 ISO, n = 7 CSL311. Data are expressed as mean ± SEM. **P* < .05, ***P* < .01, ****P* < .001 ISO vs SAL and #*P* < .05, ##*P* < .01 ISO vs CSL311 by one-way analysis of variance. *Cst*, Static compliance; *Ers*, respiratory system elastance; *i.n.*, intranasal; *ISO*, isotype; *i.v.*, intravenous; *SAL*, saline.

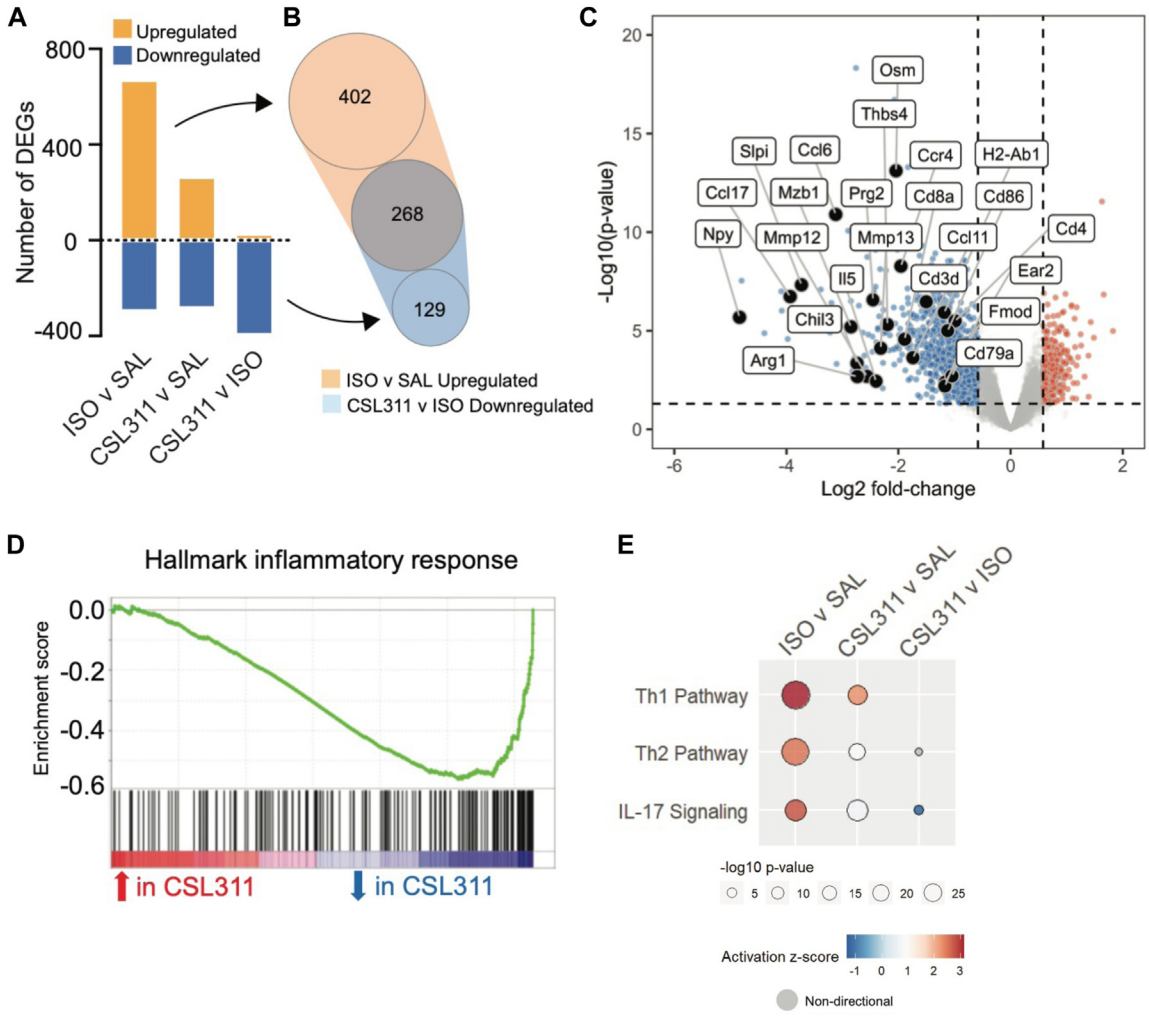

FIG 5. ASP challenge induces inflammation-associated gene expression that is normalized by βc antagonism. Mice were challenged with ASP or saline and treated with CSL311 or isotype control antibody as shown in Fig 4. At 48 hours after the last ASP challenge, the lungs were removed, and RNA was extracted before whole-transcriptome analysis by RNA sequencing. **(A** and **B)** Number of genes upregulated *(orange)* and downregulated *(blue)* are shown for the indicated comparisons. **(C)** Volcano plot showing genes differentially regulated by treatment with CSL311. **(D)** Gene set enrichment analysis of genes differentially regulated by CSL311 showing a reduction in hallmark inflammatory response genes. **(E)** Pathway enrichment analysis showing loss of T_H1, T_H2, and IL-17 pathway activation following CSL311 treatment. n = 3 SAL, n = 5 ISO, and n = 5 CSL311. *DEG*, Differentially expressed gene; *ISO*, isotype; *SAL*, saline.

genes) (Fig E3). Overall, inhibition of βc signaling resulted in broad suppression of the ECM organization Gene Ontology network (Fig E4 in the Online Repository at www.jacionline.org), and based on pathway hierarchy analysis in IPA, the key protein transcripts being targeted include *Mmp12, Mmp13,* and *Mmp19*; cathepsin lysosomal proteases *Ctsl, Ctsk,* and *Ctss*; *Lgals3* (encoding galectin-3); and *Fmod,* the gene for fibromodulin. Together, these data indicate that blocking βc cytokine signaling inhibits chronic ASP-induced airway remodeling by regulating genes involved in ECM turnover and deposition.

DISCUSSION

In addition to frontline corticosteroids, therapies targeting individual T2 mediators are now available to treat eosinophilic asthma. However, patients with a T2-low or mixed-granulocytic profile cannot be managed by T2 blockers alone.[23] Receptors and their respective ligands that converge on multiple inflammatory pathways represent an appealing therapeutic target, as they have the potential benefit of treating a broader spectrum of asthma endotypes. In this study, we identified that the expression of the βc receptor subunit shared by GM-CSF, IL-5, and IL-3 was increased in patients with severe asthma, where *CSF2RB* expression was closely associated with profibrotic gene *COL1A1* expression. We also demonstrated for the first time that βc antagonism with CSL311 simultaneously reduced T2 and neutrophilic inflammation and inhibited AHR and airway fibrosis in 2 allergen exposure models with extracts from the clinically relevant microorganisms house dust mite and *Aspergillus*. House dust mite exposure correlates with asthma symptoms,[24] and sensitization to house dust mite is associated with severe asthma.[25] *Aspergillus* sensitization also correlates with asthma,[26] with between 12% and 78% of

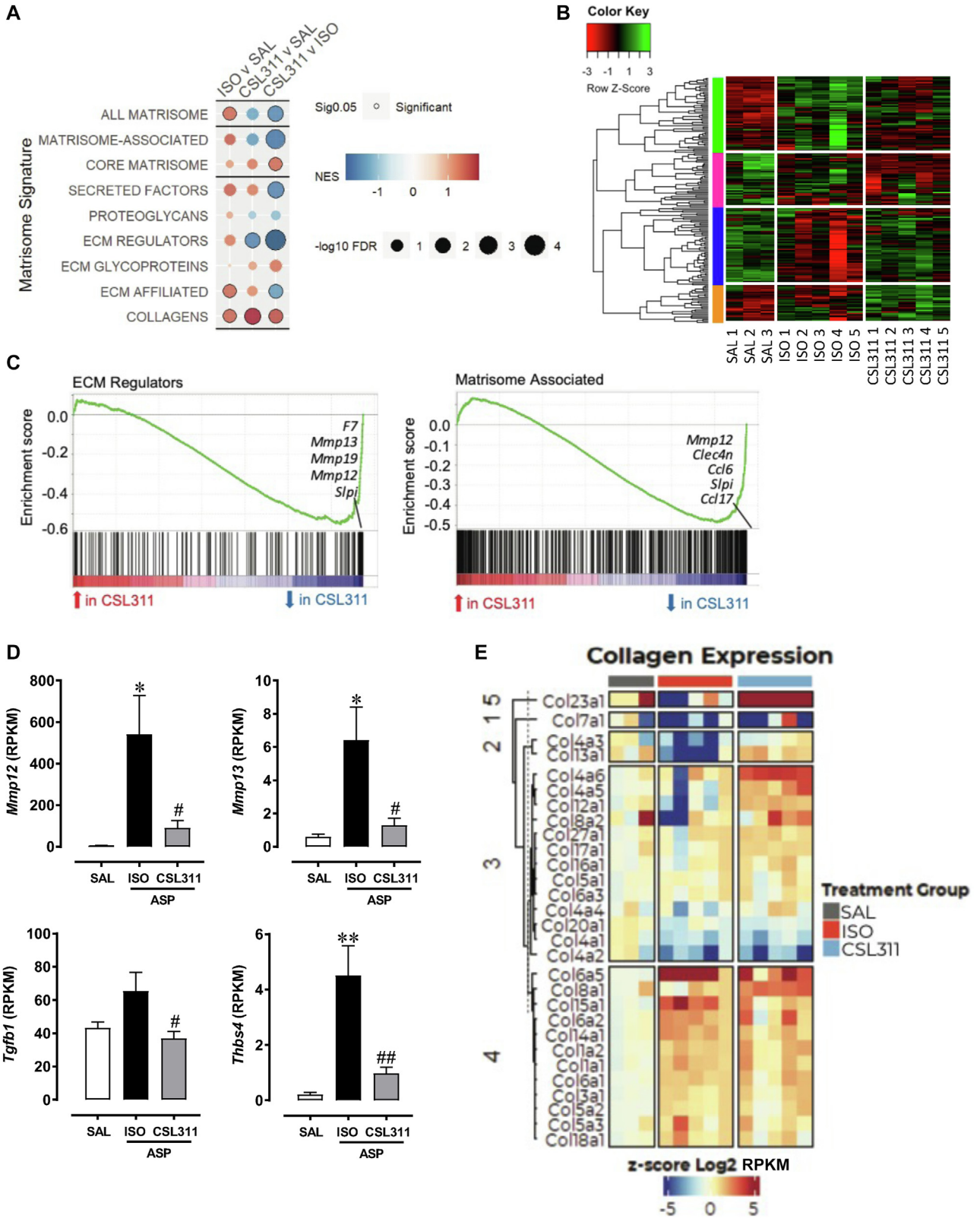

FIG 6. ASP challenge induces fibrosis-associated changes to ECM gene expression, which are normalized by βc antagonism. RNA sequencing on lung tissue following 8 weeks of ASP exposure with or without CSL311 as shown in Fig 5. **(A)** Pathway enrichment analysis of matrisome genes catalogued as shown in the labels on the left. **(B)** Heatmap representation of ECM genes ordered by unsupervised hierarchical clustering. **(C)** GSEA analysis of ECM regulators and matrisome-associated gene sets. **(D)** Bar graphs showing expression of genes involved in tissue remodeling measured by RNA sequencing. **(E)** Expression of

patients with asthma found to be sensitized to *Aspergillus* in different studies.[27] *Aspergillus* exposure also causes pulmonary fibrosis in both asthmatic patients and mouse models.[15,28]

There are currently no therapies to treat patients with severe asthma with persistent neutrophilic or mixed neutrophilic and eosinophilic inflammation. We have previously shown that blockade of G-CSF receptor selectively inhibits neutrophilic inflammation in a mouse model of influenza-driven severe asthma, although this strategy did not suppress T2 inflammation.[29] While the regulation of neutrophilic inflammation by GM-CSF is well characterized in pulmonary diseases such as chronic obstructive pulmonary disease and respiratory infection,[6,30] this axis is inadequately defined in severe asthma. In our present study, βc antagonism reduced neutrophil lung infiltration and NET formation, the latter of which may also have contributed to the observed reduction in T2 and T_H17 cytokines, as NETs have been implicated in lung recruitment of monocyte-derived dendritic cells and downstream T_H2 cell activation[31] and T_H17 cell differentiation.[32] In mice, genetic deletion of *Csf2rb* or *Gmcsfr* has been shown to block the induction of type 2 conventional dendritic cells, which preferentially activate T_H17 cells needed for promoting HDM-induced lung neutrophilia.[33] CSL311 therefore may represent an alternative and effective treatment that suppresses T_H17 signaling and lung neutrophilia. An advantage of βc antagonism is the concurrent inhibition of the monocytic population that is increasingly recognized to be pathogenic in asthma. In patients with severe, but not mild or moderate, asthma, blood monocytes were increased[34] and acquired a steroid-resistant proinflammatory profile.[35,36] Following lung recruitment, monocytes give rise to interstitial macrophages that can become alternatively activated (alternatively activated macrophages) under the influence of the T2 cytokines IL-4 and IL-13.[37,38] Interstitial macrophages are considered pathogenic, as they produce collagen[39] and promote fibroblast proliferation,[40] and their number positively correlate with lung function decline and asthma severity.[41] Fibrocytes of monocyte origin have also been shown to expand in the circulation of patients with severe asthma.[42] Consistent with these reports, we observed a marked increase in blood monocytes and lung interstitial macrophages in hβcTg mice treated with CFA-HDM. This finding was associated with prominent airway fibrosis, characterized by collagen fiber deposition and altered lung mechanics consistent with pulmonary fibrosis that are inhibited by βc signaling blockade. ASP exposure induced genes encoding collagen species known to form fibrillar structures, whereas blocking βc signaling resulted in preferential expression of nonfibrillar collagens. Airway fibroblasts and myofibroblasts produce ECM components that remodel the airway and reduce tissue elasticity via deposition of ECM components including collagen.[43] Expression of the gene encoding TGF-β1 was increased following ASP exposure and was decreased by CSL311 treatment. TGF-β1 induces collagen production by fibroblasts[44] and can be produced by both eosinophils[45] and neutrophils.[46] In addition, members of the matrix metalloproteinase, thrombospondin, and cathepsin families remodel the ECM and regulate tissue fibrosis,[47-49] several of which are upregulated by ASP exposure and inhibited by blocking βc signaling. As a major source of these proteins are cells of the myeloid lineage, it is likely that both IL-5 and GM-CSF contribute to airway remodeling via their effects on eosinophils, neutrophils, and macrophages.

In summary, our study reveals βc signaling as a major effector pathway deployed by GM-CSF and IL-5 to collaboratively drive T2 inflammation and neutrophilic inflammation in severe asthma. Antagonizing βc signaling with a single antibody (CSL311) represents a novel treatment paradigm in severe asthma, as it effectively inhibits multiple myeloid populations including interstitial macrophages, neutrophils, and eosinophils and thereby prevents pathological fibrosis and airway remodeling.

DISCLOSURE STATEMENT

This work was supported by funding from the Australian National Health and Medical Research Council (grant no. GNT1127290 to A.F.L. and grant no. GNT2004288 to A.F.L., D.J.T., and H.P.), The Hospital Research Foundation (grant no. C-MCF-02-2018-MIDC to D.J.T. and grant no. 2018-QA25222 to K.H.Y.), and CSL Limited to A.F.L. and S.B.

Disclosure of potential conflict of interest: C. Owczarek, N. Wilson, and S. P. Keam are employed by CSL Limited. The rest of the authors declare that they have no relevant conflicts of interest.

We thank Jessica Chao for assistance in the laboratory and acknowledge support of the Australian Cancer Research Foundation Cancer Discovery Accelerator. Requests for hβcTg mice can be addressed to Angel F. Lopez, MBBS, PhD, at Centre for Cancer Biology, SA Pathology and the University of South Australia, PO Box 2471, Adelaide, SA 5001, Australia, or via e-mail: Angel.Lopez@sa.gov.au.

Key messages

- **Expression of the βc receptor for cytokines IL-3, IL-5, and GM-CSF is associated with severe asthma.**
- **Signaling by the common β receptor promotes airway inflammation and fibrosis that can be blocked by the anti-βc antibody CSL311.**
- **The anti-βc antibody CSL311 normalizes fibrosis-associated ECM gene expression.**

REFERENCES

1. Agusti A, Bel E, Thomas M, Vogelmeier C, Brusselle G, Holgate S, et al. Treatable traits: toward precision medicine of chronic airway diseases. Eur Respir J 2016;47:410-9.
2. Moore WC, Hastie AT, Li X, Li H, Busse WW, Jarjour NN, et al. Sputum neutrophil counts are associated with more severe asthma phenotypes using cluster analysis. J Allergy Clin Immunol 2014;133:1557-63.e5.
3. Loza MJ, Djukanovic R, Chung KF, Horowitz D, Ma K, Branigan P, et al. Validated and longitudinally stable asthma phenotypes based on cluster analysis of the ADEPT study. Respir Res 2016;17:165.
4. Busse WW, Holgate S, Kerwin E, Chon Y, Feng J, Lin J, et al. Randomized, double-blind, placebo-controlled study of brodalumab, a human anti-IL-17 receptor monoclonal antibody, in moderate to severe asthma. Am J Respir Crit Care Med 2013;188:1294-302.
5. O'Byrne PM, Metev H, Puu M, Richter K, Keen C, Uddin M, et al. Efficacy and safety of a CXCR2 antagonist, AZD5069, in patients with uncontrolled persistent

collagen genes represented in a heatmap ordered by unsupervised hierarchical clustering. n = 3 saline, n = 5 isotype, n = 5 CSL311. Data are mean ± SEM. *$P < .05$, **$P < .01$ ISO vs SAL and #$P < .05$, ##$P < .01$, ISO vs CSL311 by one-way analysis of variance. *ISO*, Isotype; *RPKM*, reads per kilobase million; *SAL*, saline.

asthma: a randomised, double-blind, placebo-controlled trial. Lancet Respir Med 2016;4:797-806.
6. Vlahos R, Bozinovski S, Chan SP, Ivanov S, Linden A, Hamilton JA, et al. Neutralizing granulocyte/macrophage colony-stimulating factor inhibits cigarette smoke-induced lung inflammation. Am J Respir Crit Care Med 2010;182:34-40.
7. Broughton SE, Dhagat U, Hercus TR, Nero TL, Grimbaldeston MA, Bonder CS, et al. The GM-CSF/IL-3/IL-5 cytokine receptor family: from ligand recognition to initiation of signaling. Immunol Rev 2012;250:277-302.
8. Moldenhauer LM, Cockshell MP, Frost L, Parham KA, Tvorogov D, Tan LY, et al. Interleukin-3 greatly expands non-adherent endothelial forming cells with pro-angiogenic properties. Stem Cell Res 2015;14:380-95.
9. Pant H, Hercus TR, Tumes DJ, Yip KH, Parker MW, Owczarek CM, et al. Translating the biology of beta common receptor-engaging cytokines into clinical medicine. J Allergy Clin Immunol 2023;151:324-44.
10. Panousis C, Dhagat U, Edwards KM, Rayzman V, Hardy MP, Braley H, et al. CSL311, a novel, potent, therapeutic monoclonal antibody for the treatment of diseases mediated by the common beta chain of the IL-3, GM-CSF and IL-5 receptors. MAbs 2016;8:436-53.
11. Wang H, Tumes DJ, Hercus TR, Yip KH, Aloe C, Vlahos R, et al. Blocking the human common beta subunit of the GM-CSF, IL-5 and IL-3 receptors markedly reduces hyperinflammation in ARDS models. Cell Death Dis 2022;13:137.
12. Yip KH, McKenzie D, Ramshaw HS, Chao J, McClure BJ, Raquet E, et al. Targeting the human betac receptor inhibits contact dermatitis in a transgenic mouse model. J Invest Dermatol 2022;142:1103-13.e11.
13. Yip KH, Wilson NJ, Pant H, Brown CL, Busfield S, Ng M, et al. Anti-betac mAb CSL311 inhibits human nasal polyp pathophysiology in a humanized mouse xenograft model. Allergy 2020;75:475-8.
14. Wang H, FitzPatrick M, Wilson NJ, Anthony D, Reading PC, Satzke C, et al. CSF3R/CD114 mediates infection-dependent transition to severe asthma. J Allergy Clin Immunol 2019;143:785-8.e6.
15. Ichikawa T, Hirahara K, Kokubo K, Kiuchi M, Aoki A, Morimoto Y, et al. CD103(hi) Treg cells constrain lung fibrosis induced by CD103(lo) tissue-resident pathogenic CD4 T cells. Nat Immunol 2019;20:1469-80.
16. Ouyang S, Liu C, Xiao J, Chen X, Lui AC, Li X. Targeting IL-17A/glucocorticoid synergy to CSF3 expression in neutrophilic airway diseases. JCI Insight 2020;5:e132836.
17. Devos FC, Maaske A, Robichaud A, Pollaris L, Seys S, Lopez CA, et al. Forced expiration measurements in mouse models of obstructive and restrictive lung diseases. Respir Res 2017;18:123.
18. Vanoirbeek JA, Rinaldi M, De Vooght V, Haenen S, Bobic S, Gayan-Ramirez G, et al. Noninvasive and invasive pulmonary function in mouse models of obstructive and restrictive respiratory diseases. Am J Respir Cell Mol Biol 2010;42:96-104.
19. Kanehisa M, Goto S. KEGG: Kyoto Encyclopedia of Genes and Genomes. Nucleic Acids Res 2000;28:27-30.
20. Aran D, Hu Z, Butte AJ. xCell: digitally portraying the tissue cellular heterogeneity landscape. Genome Biol 2017;18:220.
21. Naba A, Clauser KR, Hoersch S, Liu H, Carr SA, Hynes RO. The matrisome: in silico definition and in vivo characterization by proteomics of normal and tumor extracellular matrices. Mol Cell Proteomics 2012;11:M111.014647.
22. Hynes RO, Naba A. Overview of the matrisome—an inventory of extracellular matrix constituents and functions. Cold Spring Harb Perspect Biol 2012;4:a004903.
23. Silkoff PE, Moore WC, Sterk PJ. Three major efforts to phenotype asthma: severe asthma research program, asthma disease endotyping for personalized therapeutics, and unbiased biomarkers for the prediction of respiratory disease outcome. Clin Chest Med 2019;40:13-28.
24. Platts-Mills TA, Erwin EA, Heymann PW, Woodfolk JA. Pro: the evidence for a causal role of dust mites in asthma. Am J Respir Crit Care Med 2009;180:109-13, discussion 20-1.
25. Sylvestre L, Jegu J, Metz-Favre C, Barnig C, Qi S, de Blay F. Component-based allergen-microarray: Der p 2 and Der f 2 dust mite sensitization is more common in patients with severe asthma. J Investig Allergol Clin Immunol 2016;26:141-3.
26. Jaakkola MS, Ieromnimon A, Jaakkola JJ. Are atopy and specific IgE to mites and molds important for adult asthma? J Allergy Clin Immunol 2006;117:642-8.
27. Knutsen AP, Bush RK, Demain JG, Denning DW, Dixit A, Fairs A, et al. Fungi and allergic lower respiratory tract diseases. J Allergy Clin Immunol 2012;129:280-91, quiz 92-3.
28. Patterson R, Greenberger PA, Radin RC, Roberts M. Allergic bronchopulmonary aspergillosis: staging as an aid to management. Ann Intern Med 1982;96:286-91.
29. Wang H, Aloe C, McQualter J, Papanicolaou A, Vlahos R, Wilson N, et al. G-CSFR antagonism reduces mucosal injury and airways fibrosis in a virus-dependent model of severe asthma. Br J Pharmacol 2021;178:1869-85.
30. Bozinovski S, Jones J, Beavitt SJ, Cook AD, Hamilton JA, Anderson GP. Innate immune responses to LPS in mouse lung are suppressed and reversed by neutralization of GM-CSF via repression of TLR-4. Am J Physiol Lung Cell Mol Physiol 2004;286:L877-85.
31. Toussaint M, Jackson DJ, Swieboda D, Guedan A, Tsourouktsoglou TD, Ching YM, et al. Host DNA released by NETosis promotes rhinovirus-induced type-2 allergic asthma exacerbation. Nat Med 2017;23:681-91.
32. Wilson AS, Randall KL, Pettitt JA, Ellyard JI, Blumenthal A, Enders A, et al. Neutrophil extracellular traps and their histones promote Th17 cell differentiation directly via TLR2. Nat Commun 2022;13:528.
33. Kim YM, Kim H, Lee S, Kim S, Lee JU, Choi Y, et al. Airway G-CSF identifies neutrophilic inflammation and contributes to asthma progression. Eur Respir J 2020;55:1900827.
34. Al-Rashoudi R, Moir G, Al-Hajjaj MS, Al-Alwan MM, Wilson HM, Crane IJ. Differential expression of CCR2 and CX3CR1 on CD16(+) monocyte subsets is associated with asthma severity. Allergy Asthma Clin Immunol 2019;15:64.
35. Berry MA, Hargadon B, Shelley M, Parker D, Shaw DE, Green RH, et al. Evidence of a role of tumor necrosis factor alpha in refractory asthma. N Engl J Med 2006;354:697-708.
36. Hew M, Bhavsar P, Torrego A, Meah S, Khorasani N, Barnes PJ, et al. Relative corticosteroid insensitivity of peripheral blood mononuclear cells in severe asthma. Am J Respir Crit Care Med 2006;174:134-41.
37. Ford AQ, Dasgupta P, Mikhailenko I, Smith EM, Noben-Trauth N, Keegan AD. Adoptive transfer of IL-4Ralpha+ macrophages is sufficient to enhance eosinophilic inflammation in a mouse model of allergic lung inflammation. BMC Immunol 2012;13:6.
38. Van Dyken SJ, Locksley RM. Interleukin-4- and interleukin-13-mediated alternatively activated macrophages: roles in homeostasis and disease. Annu Rev Immunol 2013;31:317-43.
39. Osterholzer JJ, Olszewski MA, Murdock BJ, Chen GH, Erb-Downward JR, Subbotina N, et al. Implicating exudate macrophages and Ly-6C(high) monocytes in CCR2-dependent lung fibrosis following gene-targeted alveolar injury. J Immunol 2013;190:3447-57.
40. Ploeger DT, Hosper NA, Schipper M, Koerts JA, de Rond S, Bank RA. Cell plasticity in wound healing: paracrine factors of M1/M2 polarized macrophages influence the phenotypical state of dermal fibroblasts. Cell Commun Signal 2013;11:29.
41. Melgert BN, ten Hacken NH, Rutgers B, Timens W, Postma DS, Hylkema MN. More alternative activation of macrophages in lungs of asthmatic patients. J Allergy Clin Immunol 2011;127:831-3.
42. Hung CH, Wang CC, Suen JL, Sheu CC, Kuo CH, Liao WT, et al. Altered pattern of monocyte differentiation and monocyte-derived TGF-beta1 in severe asthma. Sci Rep 2018;8:919.
43. Hough KP, Curtiss ML, Blain TJ, Liu RM, Trevor J, Deshane JS, et al. Airway remodeling in asthma. Front Med (Lausanne) 2020;7:191.
44. Kim KK, Sheppard D, Chapman HA. TGF-beta1 signaling and tissue fibrosis. Cold Spring Harb Perspect Biol 2018;10:a022293.
45. Minshall EM, Leung DY, Martin RJ, Song YL, Cameron L, Ernst P, et al. Eosinophil-associated TGF-beta1 mRNA expression and airways fibrosis in bronchial asthma. Am J Respir Cell Mol Biol 1997;17:326-33.
46. Chu HW, Trudeau JB, Balzar S, Wenzel SE. Peripheral blood and airway tissue expression of transforming growth factor beta by neutrophils in asthmatic subjects and normal control subjects. J Allergy Clin Immunol 2000;106:1115-23.
47. Frolova EG, Sopko N, Blech L, Popovic ZB, Li J, Vasanji A, et al. Thrombospondin-4 regulates fibrosis and remodeling of the myocardium in response to pressure overload. FASEB J 2012;26:2363-73.
48. Houghton AM, Quintero PA, Perkins DL, Kobayashi DK, Kelley DG, Marconcini LA, et al. Elastin fragments drive disease progression in a murine model of emphysema. J Clin Invest 2006;116:753-9.
49. Yoo Y, Choi E, Kim Y, Cha Y, Um E, Kim Y, et al. Therapeutic potential of targeting cathepsin S in pulmonary fibrosis. Biomed Pharmacother 2022;145:112245.

METHODS

Analysis of publicly available human data

RNA microarray data from BAL cells (GSE74986) were downloaded from Gene Expression Omnibus. This dataset included RNA samples obtained from 12 healthy donors, 28 patients with moderate asthma, and 46 patients with severe asthma. The Agilent Technologies (Santa Clara, Calif) signal intensity was normalized and log2 transformed using limma v3.54.2 (https://bioconductor.org/packages/release/bioc/html/limma.html) in RStudio (Posit Software, Boston, Mass).

Lung function

Respiratory mechanics were measured *in vivo* using a flexiVent system (flexiVent FX1; SCIREQ Scientific Respiratory Equipment, Montreal, Quebec, Canada). Briefly, mice were anesthetized with ketamine (125 mg/kg) and xylazine (25 mg/kg) or pentobarbital (65 mg/kg) before being tracheostomized and cannulated. Mice were then connected to the flexiVent, and baseline compliance and elastance parameters were first obtained. This was followed by the stepwise delivery of nebulized saline and increasing doses of methacholine (3-50 mg/mL) to the lungs to assess respiratory resistance.

BAL and tissue collection

After lung function testing, mice were euthanized by pentobarbital overdose. This was followed by BAL to collect BALF and BAL cells, and total cells recovered were counted using a hemocytometer. Cells were put on slides by cytocentrifugation and stained with a Hemacolor Rapid staining kit (Merck KGaA, Darmstadt, Germany) for differential cell analysis. BALF was then centrifuged to collect the cell-free supernatant for biochemical assays. Blood was drawn by cardiac puncture for hematologic analysis (CELL-DYN Emerald; Abbott Laboratories, Abbott Park, Ill). Lungs were perfused free of blood with ice-cold PBS. The superior lobe of the lungs was excised for flow cytometry analysis, and the left lobe was fixed in 10% neutral-buffered formalin for histologic analysis. The remaining lung lobes were snap-frozen in liquid nitrogen before −80°C storage.

Flow cytometry

The superior lung lobe was finely minced and digested in Liberase TM (Sigma-Aldrich, St. Louis, Mo) at 37°C with constant shaking. Single cell suspensions were prepared by passing the digested tissue through a 21-gauge needle and then a 40-μm cell strainer. This cell suspension was centrifuged and treated with ammonium-chloride-potassium red blood cell lysis buffer. After blocking with CD16/CD32 antibody, cells were stained with a myeloid cell antibody cocktail consisting of FITC-CD45, PE-Siglec F, APC-F4/80, eFluor 450-CD11b, PE/Cy7-CD11c, PerCp/eFluor710-Ly6G, and LIVE/DEAD Fixable Yellow Dead Cell Stain (Thermo Fisher Scientific, Waltham, Mass). Following staining, cells were fixed with an IC Fixation Buffer (Thermo Fisher Scientific) before being analyzed on a BD FACSAria flow cytometer (BD Biosciences, Franklin Lakes, NJ). All antibodies and reagents were obtained from Thermo Fisher Scientific unless otherwise stated. Data were analyzed with FlowJo v10.7.2 software (BD Biosciences).

Histology and immunofluorescence staining

The left lung lobe was fixed in 10% neutral-buffered formalin before being processed, paraffin-embedded, and sectioned at 4 μm. Sections were stained with hematoxylin and eosin for assessment of lung injury and MT for quantification of airway collagen. Stained whole-lung sections were scanned using a VS-120 Olympus slide scanner and Olympus cellSens Dimension software (Olympus Life Science, Waltham, Mass), or a Nanozoomer 2.0-HT slide scanner (Hamamatsu, Shizuoka, Japan) and QuPath software.[E1] Lung inflammation was scored in a blinded manner on a scale of 0 to 3 (none to severe) in peribronchial, perivascular, and interstitial/alveolar regions individually based on the degree of inflammatory cell infiltration. Morphometric evaluation of airway collagen was analyzed on a minimum of 4 bronchioles per section (100-350 μm diameter). A 30-μm band (region of interest) was circled around the subepithelial layer of the selected bronchioles. The MT-positive area was quantified within the region of interest and expressed as region-of-interest fractions.

Quantitative RT-PCR and BALF assays

Total RNA was extracted from snap-frozen lung tissue with an RNeasy kit (Qiagen, Hilden, Germany) and converted to cDNA with a High-Capacity cDNA Reverse Transcription Kit (Thermo Fisher Scientific). Quantitative PCR was performed using bioinformatically validated TaqMan Assays (Thermo Fisher Scientific). The threshold cycle values (Ct) of target genes were normalized to a reference gene (*Gapdh*), and the relative fold change was calculated using the ΔΔCt method. To measure markers of NETs, MPO activity in the BALF was determined using o-Dianisidine peroxidase substrate (Sigma-Aldrich) and dsDNA levels were quantified using a Quant-iT PicoGreen dsDNA Assay (Thermo Fisher Scientific). To assess lung injury, cell death marker lactate dehydrogenase was determined in the BALF using a Cytotoxicity Detection Kit (Sigma-Aldrich), and total protein contents were measured using a BCA Protein Assay Kit (Thermo Fisher Scientific).

RNA sequencing

RNA was purified from non-perfused mouse lungs by homogenizing freshly recovered lung tissue with a FastPrep tissue homogenizer (MP Biomedicals, Santa Ana, Calif) in Invitrogen TRIzol (Thermo Fisher Scientific) followed by phenol/chloroform extraction and then RNA cleanup using RNeasy Plus Micro Kit columns (Qiagen). Sequencing libraries were prepared using KAPA HyperPrep Kits (Roche Diagnostics, Indianapolis, Ind), and sequencing (1 × 75bp) was done on a NextSeq 500 System (Illumina, San Diego, Calif). Read quality was assessed using FastQC, and reads were mapped to the mouse reference genome mm10 using STAR aligner software.[E2] Differentially expressed genes were calculated using EdgeR software.[E3] The threshold for assignment of differentially expressed genes was set at a false discovery rate < .05 and an absolute $\log_2$ fold-change >1. GSEA was done with GSEA 4.3.2.[E4] Gene network analysis was done using IPA (Qiagen).

REFERENCES

E1. Bankhead P, Loughrey MB, Fernandez JA, Dombrowski Y, McArt DG, Dunne PD, et al. QuPath: open source software for digital pathology image analysis. Sci Rep 2017;7:16878.
E2. Dobin A, Davis CA, Schlesinger F, Drenkow J, Zaleski C, Jha S, et al. STAR: ultrafast universal RNA-seq aligner. Bioinformatics 2013;29:15-21.

E3. Robinson MD, McCarthy DJ, Smyth GK. edgeR: a Bioconductor package for differential expression analysis of digital gene expression data. Bioinformatics 2010;26:139-40.

E4. Subramanian A, Tamayo P, Mootha VK, Mukherjee S, Ebert BL, Gillette MA, et al. Gene set enrichment analysis: a knowledge-based approach for interpreting genome-wide expression profiles. Proc Natl Acad Sci U S A 2005;102:15545-50.

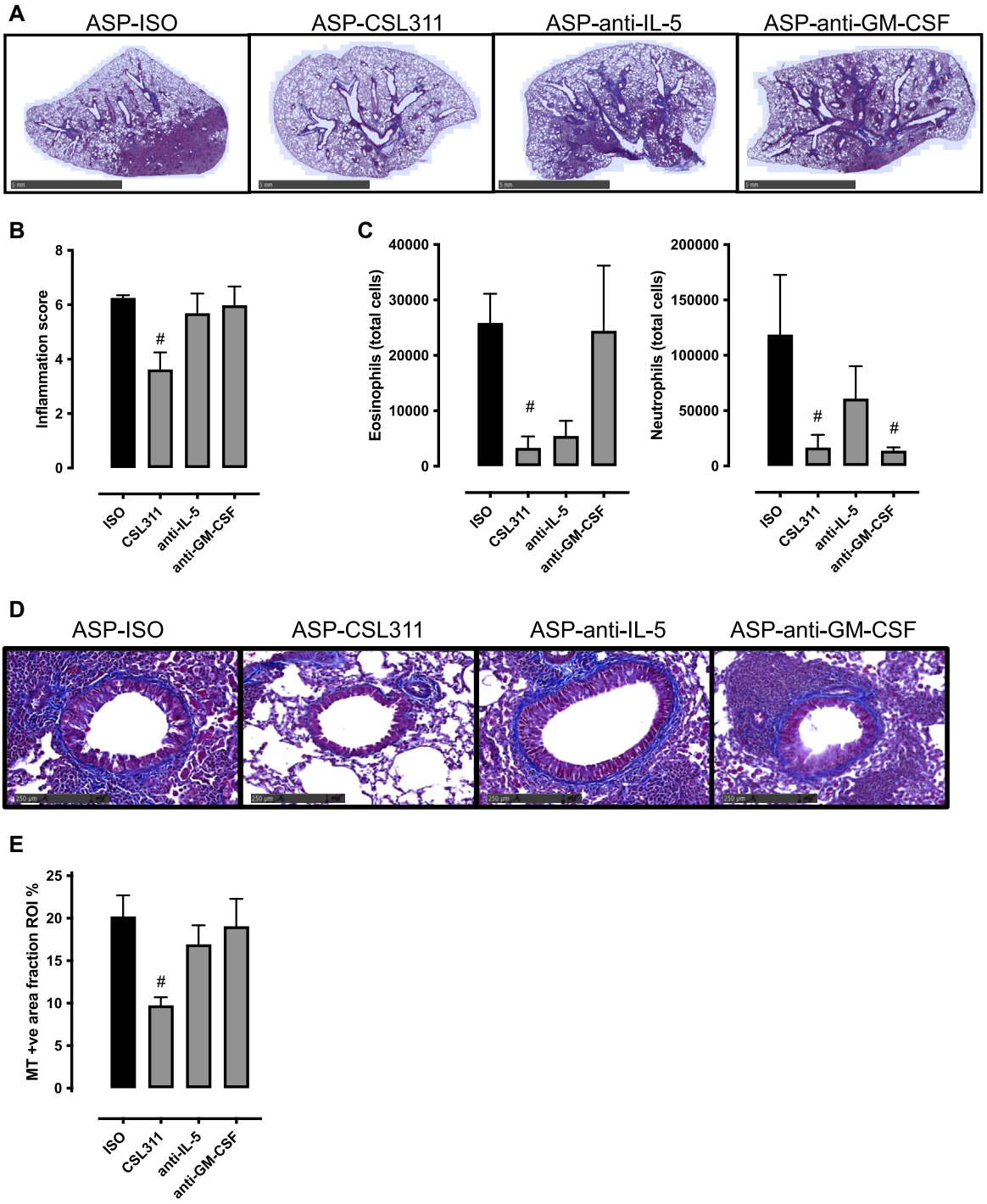

FIG E1. βc blockade provides superior protection against ASP-induced airway inflammation and remodeling compared with IL-5 or GM-CSF neutralization alone. All mice were treated with 50 μg of ASP once a week for 4 weeks followed by 20 μg of ASP twice a week for 4 weeks as shown in Fig 4, *A*. ISO, CSL311, anti-IL-5 (clone TRFK5), and anti-GM-CSF (clone MP1-229E) groups received intravenous injection of 20 mg/kg antibody via the tail vein twice a week for the final 4 weeks of the model. BAL and lung tissue recovery were done 48 hours after the last ASP challenge. **(A)** Representative whole-lung lobe images of tissue sections stained with MT. **(B)** Inflammation score. **(C)** BAL cell counts. **(D)** Collagen is stained in blue with representative images from isotype, CSL311, anti-IL-5 and anti-GM-CSF treatment groups shown. **(E)** Quantitation of collagen positive pixels. n = 4 for ISO and CSL311, and n = 5 for anti-IL-5 and anti-GM-CSF. Data are expressed as mean ± SEM. #$P < .05$, ISO vs CSL311 by one-way analysis of variance. *ISO*, Isotype; *ROI*, region of interest.

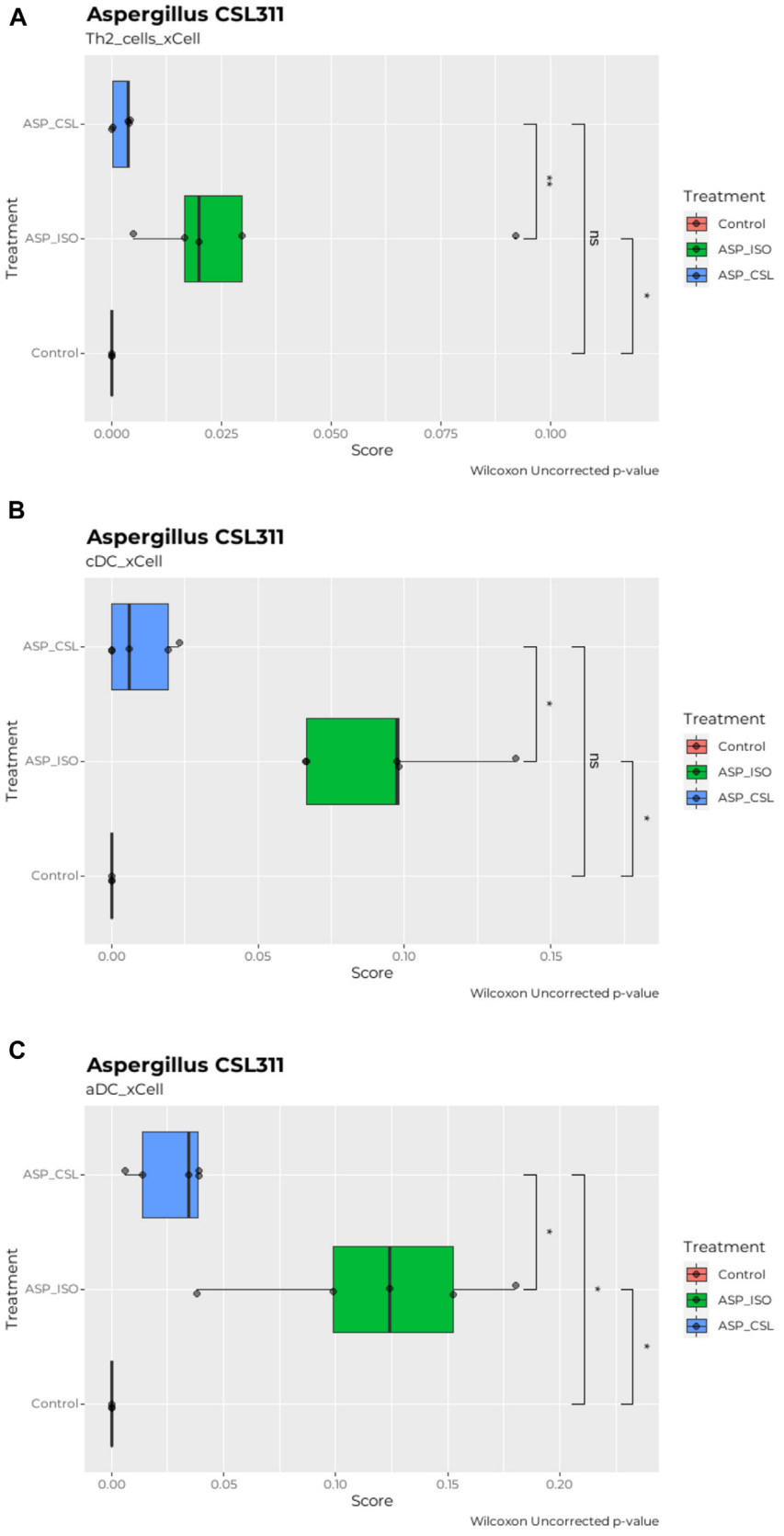

FIG E2. Prediction of cellular enrichment using xCell. (**A-C**) T_H2 cells *(A)*, conventional dendritic cells *(B)*, and activated dendritic cells *(C)*. * indicates that the cellular signature is significantly different for the indicated comparisons. From RNA sequencing data shown in Figs 5 and 6. *aDC*, Activated dendritic cells; *cDC*, conventional dendritic cells; *CSL*, CSL311; *ISO*, isotype.

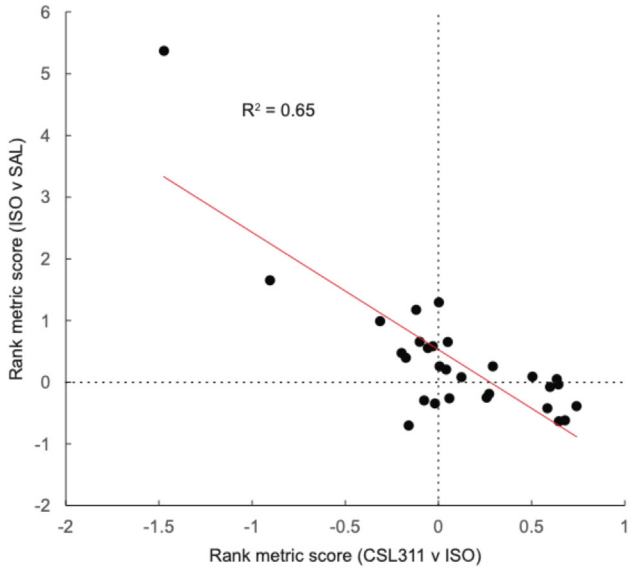

CSL311 vs ISO	*Fibril forming*	ISO vs SAL	*Fibril forming*
Col8a1	Yes	Col5a3	Yes
Col23a1	No	Col15a1	Yes
Col4a6	No	Col6a1	Yes
Col17a1	No	Col3a1	Yes
Col13a1	No	Col1a2	Yes
Col12a1	Yes	Col14a1	Yes
Col4a5	No	Col6a2	Yes
Col4a3	No	Col5a2	Yes
		Col1a1	Yes
		Col6a5	Yes

FIG E3. Collagen gene expression in mouse lung after ASP challenge. Collagen gene expression in SAL vs ISO and ISO vs CSL311 groups. From RNA sequencing data shown in Figs 5 and 6. *ISO*, Isotype; *SAL*, saline.

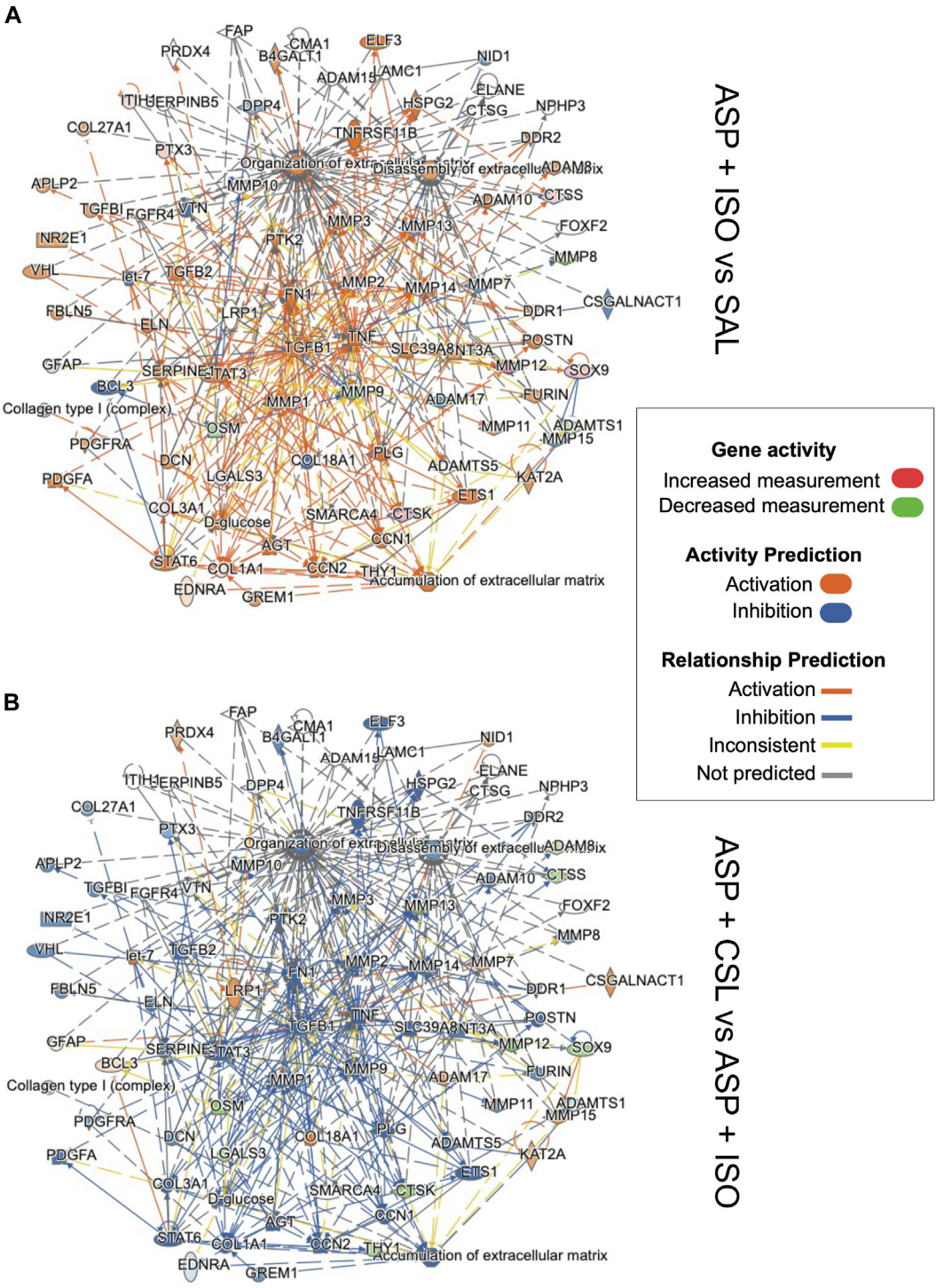

FIG E4. ECM organization gene network is suppressed by CSL311. (**A** and **B**) Network constructed based on gene ontology term: ECM organization with ASP-ISO treatment group compared with SAL control treatment *(A)* and ASP-ISO treatment group compared with the ASP-CSL311 treatment group *(B)*. The majority of the ASP-associated remodeling network is predicted to be suppressed by CSL311. From RNA-Seq data shown in Figs 5 and 6. *CSL*, CSL311; *ISO*, isotype; *SAL*, saline.